Mixed dc Electrical Conduction in Zinc Potassium Doped Borate Glasses

Prashant Kumar M[1], Arunkumar V. Banagar[1*], N. Nagaraja[2]

[1]*Department of Physics, Government College (Autonomous), Kalaburagi, Karnataka, India*
[2]*Department of Physics, Rao Bahadur Y. Mahabaleswarappa Engineering College Ballari, Karnataka, India*
Email: banagararun@gmail.com

Received: 12 Feb 2025 Revised: 18 March 2025 Accepted: 20 April 2025

Abstract: A series of borate glass system in the composition (K2O) x -(ZnO)0.5-x-(B2O3)0.5; x=0.08,0.16,0.24,0.32 and 0.40 has been prepared using melt quench technique. The samples were annealed at 453K, to remove any thermal strains present in the glass matrix. The XRD pattern confirms the non-crystalline nature of the glass systems. The room temperature density of the glass samples was measured by adopting Archimedes principle and molar volume estimated. The oxygen packing densities were calculated using molar volume. The room temperature density and molar volume varied non-linearly and appositively with mole fraction of K2O. DC electrical conductivity was estimated in the temperature range 313 K to 473 K by using two probe method. The high temperature activation energy was calculated for T >θD/2 in the light of Mott's small polaron hopping model. Various small polaron hopping parameters such as small polaron radius, effective dielectric constant, polaron band width, optical phonon frequency, small polaron coupling constant, density of states at Fermi level have been calculated and discussed. The nonlinear variation of conductivity and activation energy with mole fraction of K2O shows the changeover of conduction mechanism taking place in present series of glasses at x=0.24. It is for the first time that two dominant conduction mechanism regimes were observed in potassium-zinc-borate glass systems.

Keywords: Borate Glasses; Electronic conductivity; Ionic conductivity; TMI& alkali ions; Mixed conduction; Motts SPH model IM, underground construction, restructuring, repair, operation, project integration, prefabricated construction

1. Introduction

Borate glasses doped with transition metal and alkali ions are considered as an important class of materials in the applications of microelectronics, optics, optical fibres, electrodes, solid electrolytes in batteries and other electrochemical devices [1-3].The borate glasses have attracted the attention of many researchers due to their good mechanical hardness, high spectral transparency, low melting temperature, outstanding thermal stability and affinity of B-O groups to coordinate either trigonally$(BO_3)^{3+}$ or tetrahedral $(BO_4)^{3+}$ in the glass matrix [4-6].Many researchers reported the effect of modifier such as K^+ ions on physical properties, transport properties, viscosity and melting points of oxide glass systems by altering the glass network and generating non-bridging oxygens [7,8]. Alkali rich containing oxide glasses exhibit dominant ionic conduction and the conductivity is reported to be due to migration of alkali ions from one ionic site to another ionic site in the glass matrix [9,10].The electrical conductivity in transition metal (TM) ions doped oxide glasses is due to hopping of charge carriers between multivalent states of TM ions i.e. from low valance state to high valence state [11-13].Borate glasses doped with zinc plays a dual nature such as glass former and network modifier. The glasses containing

zinc are reported to exhibit semiconducting property, better stability, moisture resistance, transparency and low rate of crystallization [14,15]. Both alkali and TM ions doped oxide glass systems exhibit mixed electrical conduction due polarons and alkali ions [11,16]. Electronic conductivity in these types of glasses vary substantially with the alkali content exhibiting minima at certain alkali content [17,18]. Mixed conduction was reported to occur in many of borate glasses doped with alkali and transition metal ions [19,20]. Researchers reported the changeover of conduction mechanism from ionic to electronic or vice versa in many of the oxide glass systems [20,21]. However, the deep minima or peak observed in terms of many physical parameters with mole fractions of alkali content is different for different glass systems [22,23].

The present paper reports the experimental results on room temperature density, molar volume, temperature dependent dc electronic conductivity, high temperature activation energy and other polaron related parameters in the glass systems

$(K_2O)_x$-$(ZnO)_{0.5-x}$-$(B_2O_3)_{0.5}$; x=0.08, 0.16, 0.24, 0.32 and 0.40 labelled as BZK8, BZK16, BZK24, BZK32 and BZK40.

The main aim and objective of the present work is to understand the dominant conduction mechanism with mole fractions of K_2O in the present series of glass systems and physics involved in it.

2. Experimental

The glass samples were prepared by adopting melt-quench technique. The analytical reagent grade chemicals with 99.99% purity, such as K_2CO_3, ZnO and H_3BO_3 procured from Sigma-Aldrich were used for synthesis of the glass samples. The chemicals were weighed in appropriate ratios using a single pan digital balance (model Scale Tech 623-CL with an accuracy of 0.1 mg) and thoroughly mixed by manually grinding them in an agate mortar before transferring the mixture to porcelain crucibles. The mixture was heated gradually to 1300K in an electrical muffle furnace at which the melt was formed. When the homogeneous colourless liquid was obtained, the melt was then suddenly poured on to a thick stainless-steel plate and by pressing with another similar steel plate onto it. The random sized glass samples were collected. In order to remove thermal strains, if any, the samples were annealed at 473K.

All the prepared glass samples were subjected to X-ray diffraction studies. The X-ray diffraction pattern of all samples were taken using Cu-Ku radiation of wavelength 1.4518 Å in X-ray diffractometer type ultima IV (Rigaku, Japan).

The densities of the glass samples at room temperature were measured by Archimedes principle, using toluene (density = 0.8966 g/cc) as an immersion liquid [24].

$$D = \left(\frac{W_{air}}{W_{air}-W_L}\right) D_L \quad g/cm^3 \qquad (1)$$

where, W_{air} is the weight of the glass samples in air, W_L is the weight of the sample in toluene and D_L is the density of toluene. The error on the measured density was estimated to be within ±2%. The molar volume (V_m) of the prepared glass samples was calculated from the density data using the following expression [24].

$$V_m = \frac{\sum x_i M_i}{\rho} \qquad (2)$$

where, M_i is the molecular weight of the glass composition, x_i mole fractions of the various constituents, and ρ is the density of the glass.

The glass samples were well dimensioned into appropriate size and shape of thickness 2mm to 4 mm and cross-sectional area ranging from 70 mm^2 to 80 mm^2. The dc electrical resistivity was measured in the temperature range 313K to 473K using two probe instruments by painting silver electrodes on to two major surfaces of the glass samples. By keeping voltage across the sample constant, the current was measured by a digital picoammmeter (Make: SES Instruments, India) to an accuracy of ±1pA. Temperature of the glass samples was measured by a chromel-alumel thermocouple to an accuracy of ±1K. The conductivity of the glass samples was calculated using $\sigma = \frac{1}{\rho}$ where ρ is the resistivity given by $\rho = \frac{RA}{d}$[25], 'R' is the resistance, 'A' is the cross-sectional area and 'd' is the thickness of the glass sample. The estimated errors on conductivity were found to lie in the range 2-3%.

3. Results and Discussions

3.1 XRD

The X-Ray Diffraction patterns for all samples were depicted in Fig. 1. The broad humps over a small region of 2θ without any sharp peaks confirm the non-crystalline nature of the present glass samples.

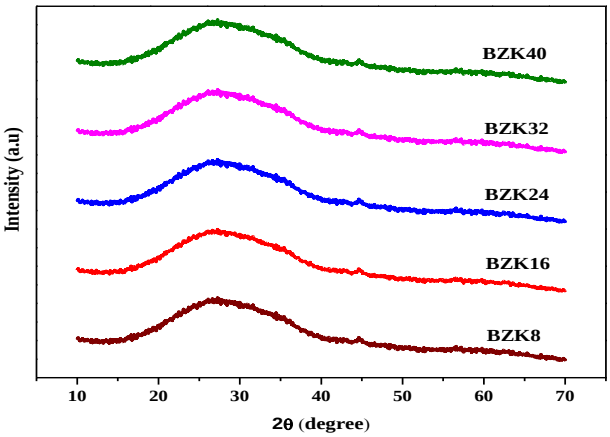

Fig.1. X-ray diffraction profile of BZK glass samples.

3.2. Density, molar volume and oxygen packing density

The room temperature density, ρ, of the present glass systems were found to be in the range 1.80 to 3.26 g/cm^3.The room temperature density decreases up to 0.24mole fraction of K_2O and then increases for further increase of K_2O content. The density values were found to be similar with those of borate glasses reported elsewhere [26,27]. The molar volume, V_m was calculated using equation (2) and found to be in the range 24.20 to 47.61 cm^3/mol. These values are comparable to that of the reported values for other borate glass systems [28]. The variation of density, ρ, and molar volume, V_m of the present series of glasses as a function of alkali concentration K_2O can be divided into two sections as illustrated in Fig. 2 and Table 2. In the first section, with K_2O content up to 0.24 mole fraction, V_m gradually increases due to the creation of excess free volume and the glass structure becomes more open. In the second section, 0.24 <x< 0.4 mole fraction of K_2O, the molar volume decreases, which is the signature of structural changes taking place in the topology of glass network hinting at the network getting closely packed [29,30].

Table 1. Batch composition of $(K_2O)_x$-$(ZnO)_{0.5-x}$-$(B_2O_3)_{0.5}$ glass system.

Glass Code	B_2O_3 (mol%)	ZnO (mol%)	K_2O (mol%)
BZK8	0.5	0.42	0.08
BZK16	0.5	0.34	0.16
BZK24	0.5	0.26	0.24
BZK32	0.5	0.18	0.32
BZK40	0.5	0.10	0.40

Table 2. Physical properties of BZK series glass system.

Glass Code	D (±0.023) (g/cm^3)	V_m (±0.030) (cm^3/mol)	OPD (±0.05) (g. atm/L)	N (x 10^{21} cm^{-3})	R (±0.02) (nm)	θ_D (K)	ν_o (x10^{13} Hz)
BZK8	3.262	24.208	82.617	3.652	3.674	686	1.429
BZK16	2.614	31.536	63.420	1.997	4.244	696	1.450
BZK24	1.804	47.617	42.002	7.985	5.251	694	1.446
BZK32	2.115	42.254	47.332	9.043	5.629	724	1.508
BZK40	2.279	40.735	49.098	8.423	6.679	714	1.487

Table 3. Polaron hopping parameters of BZK series glass system.

Glass Code	W (eV) (±0.05)	σ (Ω^{-1} m^{-1}) at 443 K (±0.02)	W_H (eV)	ε_p	r_p (nm)	J (eV)	N(E_F) x10^{21} (eV^{-1} m^{-3})	γ_p
BZK8	1.150	2.397 x10^{-5}	1.150	1.473	1.478	0.0032	5.54	38.911
BZK16	1.516	1.363 x10^{-6}	1.517	0.966	1.707	0.0024	4.74	50.588
BZK24	1.564	2.173 x10^{-7}	1.565	0.757	2.112	0.0014	2.58	52.333

BZK32	1.509	2.347 x10^{-6}	1.510	0.732	2.265	0.0012	2.02	48.401
BZK40	1.262	1.433 x10^{-5}	1.262	0.738	2.687	0.0007	1.01	41.028

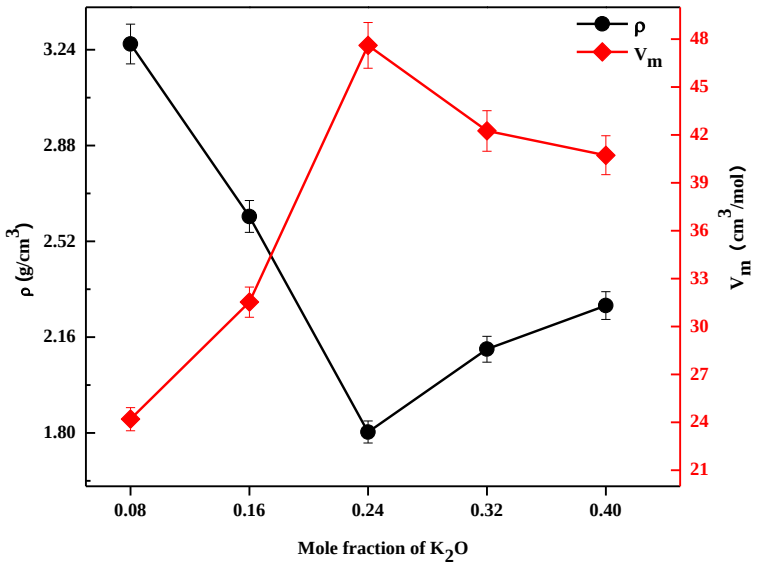

Fig. 2. Plot of density (ρ) molar volume (V_m) as a function of K2O for BZK series glasses.

The organization of oxygen atom in the oxide glasses is determined from the oxygen packing density (OPD). The oxygen packing density can be calculated from the following relation [31].

$$OPD = \frac{1000(O)}{V_m} \quad (3)$$

where 'O' represents the number of oxygen's present in the glass.

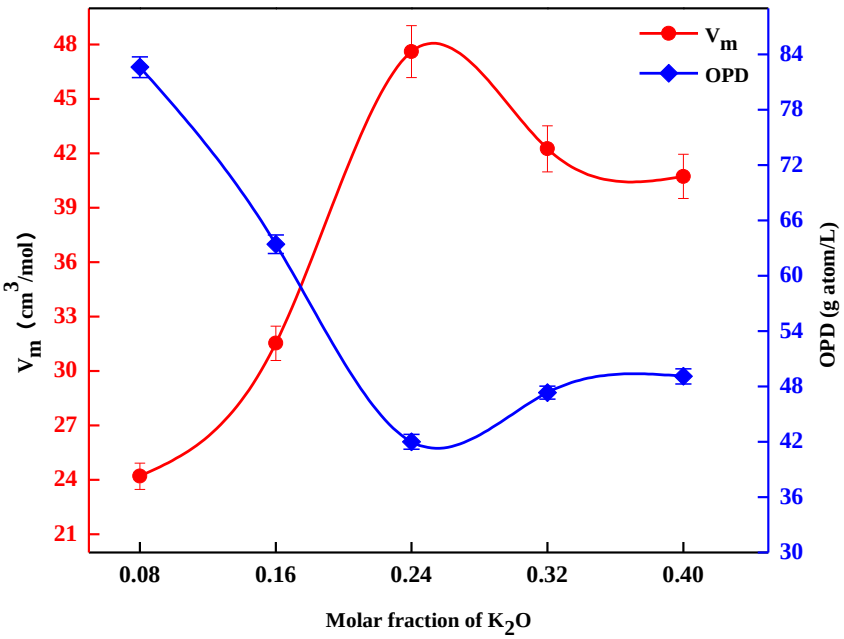

Fig. 3. Compositional variation of molar volume (V_m) and OPD with molar fraction of K2O

Fig. 3 illustrates the compositional variation of molar volume, V_m, and oxygen packing density with K_2O mole fractions. It is observed that in Table 2 and from Fig. 3 the molar volume V_m and OPD varied non-linearly with mole fraction of K_2O.The values were found to vary from 82.61 to 49.09 g. atm/L. The variation of OPD with mole fractions of K_2O in the glass matrix can be described by greater or lesser linkages with K_2O ions in the glass network [32].

3.3. DC Conductivity

In the present series of glass systems, the measured dc electrical conductivity in the temperature range from 313K to 473K was in the range from 10-5 Ω-1m-1 to 10-7 Ω-1m-1. These values are in close agreement with the dc conductivity data for other similar type of glass systems doped with alkali and TM ions [33, 34]. The temperature dependence of dc conductivity was observed to be of semiconducting in nature. The conductivity decreased with increase in mole fractions K2O up to 0.24 and then it increased for further increase in K2O content. The conductivity values for the present series of glass systems at 443K are recorded in Table 3.

The electrical conductivity in non-adiabatic regime is given by Mott's small polaron hopping (SPH) model [35],

$$\sigma = \left(\frac{\sigma_o}{T}\right) \exp\left(\frac{-W}{k_B T}\right) \quad (4)$$

where W is the activation energy and σ_ois the pre-exponential factor given as,

$$\sigma_O = \upsilon_O N e^2 R^2 C(1-C) \exp(-2\alpha R)/K_B \quad (5)$$

where, $\upsilon_o=\theta_D K_B/h$ is the optical phonon frequency [36], $\theta_D=2T$, which is Debye's temperature, N is the concentration of TMI, R is the mean spacing between TMI given as $R=N^{-1/3}$, α is the tunnelling factor and C is fraction of reduced TMI concentration to that of total TMI concentration. For the present series of glass systems, the values of N, R, θ_D and υ_o were estimated and presented in Table 2. The ln(σT) versus (1/T) plots were made for the present glass systems by fitting the conductivity data to equation (4) and presented in Fig. 4. The curves were found linear at high temperature regime i.e., for $T > \theta_D/2$ and non-linear at low temperature regime i.e., for $T< \theta_D/2$. In the high temperature regime, for $T > \theta_D/2$, the conductivity varied linearly with temperature is the characteristic of small-polaron hopping conduction mechanism [37]. The general behaviour of the curves is similar to that of other similar borate glasses doped with alkali and transition metal ions reported elsewhere [38,39]. The least square lines were fit to the data corresponding to the high temperature regime above $T > \theta_D/2$. For the best fit to ln(σT) versus (1/T) plot, the correlation coefficient r^2 values were between 0.9965 and 0.99816. From the slope of linear fits of the plots, the high temperature activation energy, W, were determined for all the glass samples and listed in Table 3. The activation energies for the present glasses were found in the range from 1.150eV to 1.564eV. The values of activation energies for the present glasses are in close agreement to those reported similar glass systems in the literature [40,41].

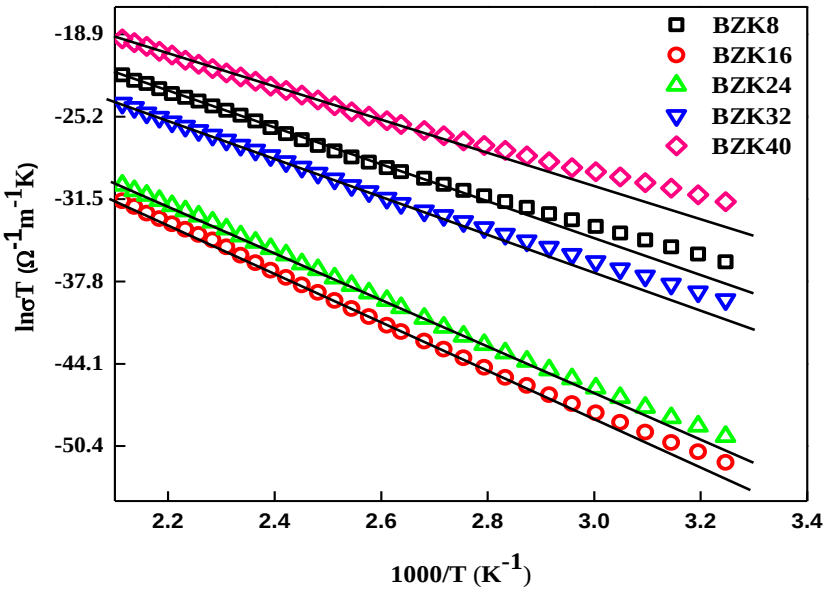

Fig. 4. Plot of ln (σT) vs 1/T of BZK glasses. Solid lines are the least square fits to the high temperature data.

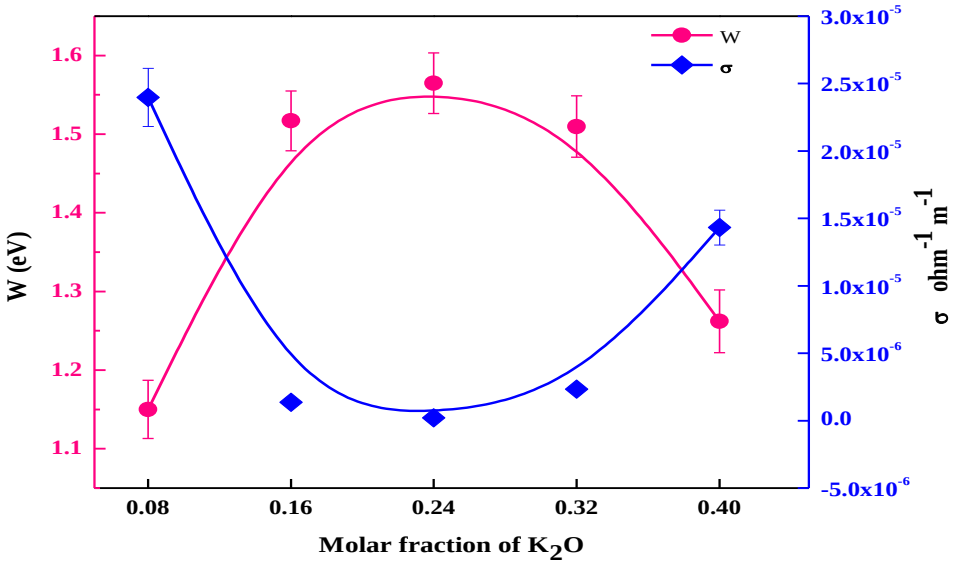

Fig.5. Compositional dependence of high temperature activation energy, W and conductivity, σ, at 443 K.

Fig. 5 shows the behaviour of dc electrical conductivity, σ, at 443K and high temperature activation energy, W, as a function of K_2O concentration. From Fig. 5, it is suggested that for $0.08 \leq x \leq 0.40$ mole fraction, the electrical conduction is due to both small polaron hopping between low and high valence states of Zn ions and migration of K^+ ions in the glass network. In the mixed dominant conduction regime polaronic and ionic conductivities are not possible to distinguish. There is a race between the polarons and K^+ ions in the glass matrix to contribute for total electrical conduction in the present glass system. For $x< 0.24$ mole fractions of K_2O the conduction was dominated by polarons and for $x>0.24$ the conductivity dominated by K^+ ions. At $x= 0.24$ mole fractions of K_2O the conductivity switch over from polaronic dominant regime to ionic dominant regime. Similar observations have been reported for many other glass systems in the literature [42,43]. In the present series of glasses, the variation of composition dependent conductivity can be attributed to cation-polaron correlation effect [44,45]. Therefore, it can be observed that the cationic conductivity commences to increase for $x > 0.24$ K_2O mole fraction of K_2O. From the above discussion, it can be concluded that a changeover of conduction mechanism taking place in the present series of glass systems predominantly from electronic to ionic at 0.24 mole fraction of K_2O [46,47].

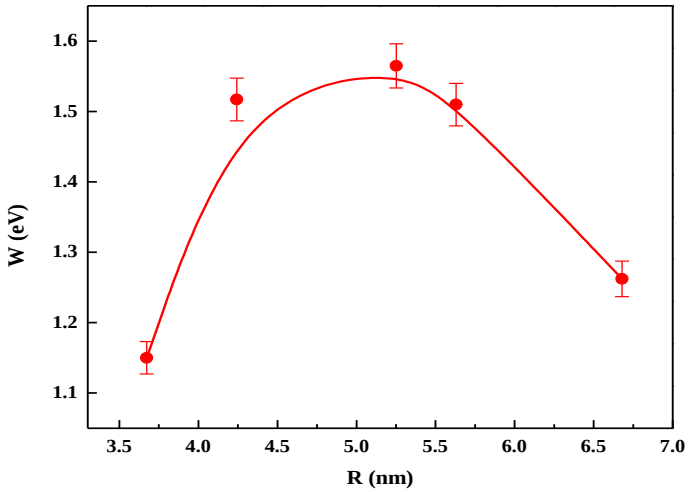

Fig. 6. Effect of mean Zn-ion spacing, R, on activation energy, W, for different glass Compositions. Lines drawn are the guides to the eye.

The relationship between the activation energy, W and the mean distance, R, between Zn ions is depicted in Fig. 6 and suggest that as ZnO content decreases, the mean distance between Zn ions increases up to 0.24 mole fraction of K_2O content and decreased for further increase in K_2O content. It is implicit that this causes W to increase and dc conductivity, σ, to decrease (Fig.4). This reveals that up to K_2O content of 0.24 mole fraction the electronic conductivity was dominant over ionic and ionic conduction is dominant over electronic for higher concentration of alkali and suggesting it may due to a switch over of predominance of conduction mechanism from electronic to ionic. Assuming that conductivity is due to hopping of electrons from Zn^+ to Zn^{2+} states up to 0.24 mole fraction and further it is dominated by K_2O cations for higher concentration.

3.4 Small polaron hopping parameters

Austin and Mott proposed that for strong electron-phonon interaction the activation energy in the high temperature region where nearest neighbour thermally activated hopping predominates the polaron hopping energy W_H and disorder energy W_D and the activation energy is given by [48],

$$W = W_H + W_D/2T > \theta_D/2$$
$$\cong W_D T < \theta_D/4 \quad (6)$$

Where $W_H(= W_P/2)$ is the polaron hopping energy and W_D is the disorder energy arising from the energy difference of the neighbours between two hopping sites.

The polaron hopping energy W_H can be calculated using following relation [49],

$$W_H = \frac{W_P}{2} = \frac{e^2}{4\varepsilon_p}\left(\frac{1}{r_p} - \frac{1}{R}\right) \quad (7)$$

Where W_P is the polaron binding energy, ε_p is the effective dielectric constant and which can be determined from the below relation [50].

$$\varepsilon_p = \frac{e^2}{4Wr_p} \quad (8)$$

where, e is the charge of the electron, w if the activation energy, and r_p is the small polaron radius which is estimated from the relation [50].

$$r_p = \left(\frac{1}{2}\right)\left(\frac{\pi}{6N}\right)^{\frac{1}{3}} \quad (9)$$

The estimated values of ε_p,r_p, are tabulated in Table 3 and similar to reported values in literature for other similar glass systems [51].

According to SPH model, the polaron bandwidth J is given by [52],

$$J > (2KTW_H/\pi)^{\frac{1}{4}}(h\upsilon_o/\pi)^{\frac{1}{2}} \quad \text{for adiabatic SPH}$$
$$J < (2KTW_H/\pi)^{\frac{1}{4}}(h\upsilon_o/\pi)^{\frac{1}{2}} \quad \text{for non-adiabatic SPH} \quad (10)$$

The polaron bandwidths above T= $\theta_D/2$ were estimated using the relation $J = J_O \exp(-\alpha R)$, where $J_O = \frac{W_{H(min)}}{4}$ [52] and were listed in Table 3. From the literature quoted for many TMI doped oxide glasses the value of α was taken 20 nm^{-1}[35, 52]. From Table 3, it can be noted that J for all glasses are found to be in the range from 0.0032eV to 0.000726eV satisfies the conduction for non-adiabatic conduction given in Eq. (10) and Holstein's condition $J<W_H/3$ for small polaron formation [52].

For the present series of glass systems, the small polaron coupling constant, γ_p, is a measure of electron-phonon interaction listed in Table 3 and was calculated from the relation, $\gamma_p = 2W_P/\hbar\upsilon_o$ where W_P polaron binding energy and is approximately given by $W_P = 2W_H$ and $\hbar = h/2\pi$, $\upsilon_o = \omega/2\pi$ [53]. It is noticed that γ_p and conductivity vary non-linearly and reaches respectively maximum and minimum value at x = 0.24. This behaviour hints at, with increase in K_2O concentration, the electron-phonon interaction becomes stronger which in turn reduces the electronic contribution to the total conductivity. In the present series of glass systems, it may be concluded that the electronic conductivity was predominant over ionic conductivity up to 0.24 mole fraction of K_2O content and the ionic conductivity was predominant over electronic conductivity for further increase in K_2O content.

The density of states at the Fermi level $N(E_F)$ were calculated using the equation $J = e^3 N(E_F)^{1/2}/\varepsilon_p^{3/2}$[53]. The estimated values of $N(E_F)$ are listed in Table 3, and they are of the order of $10^{21} eV^{-1}m^{-3}$. These $N(E_F)$ values are in agreement with the reported values for many TMI doped other oxide glass systems [52,53].

4. Conclusion

A novel series of borate glasses doped with ZnO and K_2O were prepared by melt quench technique. The XRD studies confirmed non-crystalline nature of the glass samples. The measured room temperature

density reached minimum value and the molar volume reached maximum value at x=0.24 mole fraction of K_2O concentration. This kind of behaviour is attributed to the structural changes occurring in the glass network at around x=0.24 mole fractions of K_2O.The molar volume and oxygen packing density (OPD) were estimated and their behaviour was discussed.

The dc electrical conductivity was measured in the temperature range 313K to 473K. The dc conductivity was observed to be decreasing up to 0.24 mole fractions of K_2O and increased for further increase in K_2O concentration. The high temperature conductivity data has been analysed in the light of Mott's small polaron hopping (SPH) model. The electrical conductivity decreased to minimum value and activation energy increased to maximum value with increase of mole fraction of K_2O up to x=0.24. In the present study, at x=0.24 mole fraction of K_2O, a changeover of conduction mechanism is taking place from predominantly electronic to ionic. The high temperature activation energy was determined for temperature $T > \theta_D/2$ as per as Mott's SPH model. Various small polaron hopping parameters such as small polaron radius, effective dielectric constant, polaron band width, optical phonon frequency, and electron-phonon coupling constant have been estimated and discussed.

References

1. Y.M. Moustafa, G. El-Damrawi, and M.S. Meikhail (1993) Mans.Sc. Bull.C (Nat.Sc), 20 71.
2. K. Singh and J.S. Ratnam (1988) Solid State Ionics 31 221.
3. Y. Yito, K. Miyauchiand and T. Oi (1983) J. Non-Cryst. Solids 57 389.
4. G. Kaur, M. Kumar, A. Arora, O.P. Pandey and K. Singh (2011) J. Non-Cryst. Solids 357, 858.
5. G. Kaur, O.P. Pandey and K. Singh (2012) J. Non-Cryst. Solids 358 2589.
6. E. Kaewnuam, N. Wantana, H.J. Kim and J. Kaewkhao (2017) J. Non-Cryst. Solids 464 96.
7. G. Lakshmi Narayana, K.M. Kaky, S.O. Baki, A. Lira, P. Nayar, I.V. Kityk and M.A. Mahdi, J. Alloys Compd. 690, 799 (2017).
8. Y.S.M. Alajerami, S. Hashim, W.M.S.W. Hassan, A.T. Ramli and A. Kasim (2012) Int. J. Mod. Phys. B 26 1250116/1–13.
9. T. RaghavendraRao, Ch. Venkata Reddy, Ch. Rama Krishna, D.V. Sathish, P.N. Murthy, P.S. Rao and R.V.S.S.N. Ravikumar (2012) Mater. Res. Bull. 47 2646.
10. M. Prashant Kumar, T. Sankarappa (2008) Solid State Ion 178 1719.
11. M.M. El-Desoky (2005) J. Non-Cryst. Solids 351 3139.
12. M.M. El-Desoky, M.S. Al-Assiri (2007) Mater. Sci. Eng., B 137 237.
13. C. Narayana Reddy, R.P. Sreekanth Chakradhar (2007) Mater. Res. Bull. 42 1337.
14. A.M. Abdelghany, F.H. ElBatal, H.A. ElBatal (2014) Appl. Ceram. 8 (4) 185.
15. H. Nasu and N. Soga (1982) J. Non-Cryst. Solids 53 123.
16. M.S. Meikhail and A.M. Abdelghany (2017) Silicon 9 895.
17. G.D.L.K. Jayasinghe, M.A.K.L. Dissanayake, M.A. Careem and J.L. Souquet (1997) Solid State Ion 93 291.
18. B. Eraiah, R.V. Anavekar (2001) Phys. Chem. Glasses 42 121.
19. S. Dhaiya, R. Punia, S. Murugaval and A.S. Maan (2016) Solid State Sci., 55 98.
20. M. Saad, W. Stambouli, N. Sdiri and H. Elhouichet (2017) Mater. Res. Bull., 89 224.
21. A. Bunde, M.D. Ingram and P. Maass (1994) J. Non-Cryst. Solids 1222 172.
22. E. Mansour, Y.M. Moustafa, G.M. El-Damrawi, et al (2001) Physica B, 305 242.
23. S. Ibrahim, M. M. Gomaa and H. Darwis (2014) J. Adv. Ceramics 3 155.
24. M. Prashant Kumar and T. Sankarappa (2008) Mater. Sci., 26 (3) 647.
25. T. RaghavendraRao, Ch. Venkata Reddy, Ch. Rama Krishna, D.V. Sathish, P.N. Murthy, P.S. Rao, R.V.S.S.N. Ravikumar (2011) Mater. Res. Bull. 46 2222.
26. T. RaghavendraRao, Ch. Venkata Reddy, U.S. Udayachandran Thampy, Y.P. Reddy, P.S. Rao, R.V.S.S.N. Ravikumar (2011) Spectrochim. Acta, Part A, 79 1116.
27. E. Mansour (2011) J. Non- Cryst. Solids 357 1364.
28. F. Berkemeier, S. Voss, W. Arpad, Imre and H. Mehrer (2005) J. Non-Cryst. Solids 351 3816.
29. M.M. Umair and A.K. Yahya (2013) Mater. Chem. Phys 142 549.
30. V.C. Veeranna Gowda (2013) Physica B, 426 58.
31. Y.F. Li, T.L. Zhang, J.G. Zhang and K.B. Yu (2003) J. Chem. Sci., 58 (12) 1171.
32. M.M. El-Desoky and M.Y. Hassaan (2002) Phys. Chem. Glasses 43 (1) 1.
33. A. Al-Shahrani, A. Al-Hajry and M.M. El-Desoky (2003) Phy. Status Solidi (a) 200 (2) 378.
34. N.F. Mott (1968) J. Non-Cryst. Solids 1 1.

35. H. Sakata, K. Sega and B.K. Chaudhari (1999) Phys. Rev. B 60 (5) 3230.
36. K. Sega, Y. Kuroda and H. Sakata (1998) J. Mat. Sci. 33 138.
37. A. Dutta and A. Ghosh (2005) J. Non-Cryst. Solids 351 203.
38. W. Arpad, Imre, V. Stephan and M. Helmut (2004) J. Non-Cryst. Solids 333 231.
39. B. Shanmugavelu, V.V. Ravi Kanth Kumar (2013) Solid State Sci., 20 59.
40. A. Langar, N. Sdiri, H. Elhouichet and M. Ferid (2014) J. Alloys Compd. 590 380.
41. R.A. Montani, A. Lorente and M.A. Vincenzo (2000) Solid state Ion 130 91.
42. M. Dawy and A.H. Salama (2001) Mater. Chem. Phys 71 137.
43. H.M.M. Moawad, H. Jain, R. El-Mallawany, T. Ramadan and M. El-Sharbiny (2002) J.Am. Crem.Soc, 85 (11) 2655.
44. B.V.R. Chowdari and P.P. Kumari (1998) J. Mater. Sci, 33 3591.
45. M. Sayer, A. Manshingh (1972) Phys. Rev. B, 6 4629.
46. H. Mori, H. Motsuno, H. Sakata, (2000) J. Non-Cryst. Solids 276 215.
47. M. Saad, W. Stambouli, N. Sdiri and H. Elhouichet (2017) Mater. Res. Bull, 89 224.
48. H.W. Guo, X.F. Wang, Y.X. Gong and D.N. Gao (2010) J. Non-Cryst. Solids 356 2109.
49. I.G. Austin, N.F. Mott, Adv. Phys, 18, 41 (1969).
50. M. Pal, K. Hirota, Y. Tasujigami and H. Sakata, J. Phys. D: Appl. Phys, 34, 459 (2001).
51. A. Mogus-Milankovic, D.E. Day, B. Santic (1999) Phys. Chem. Glasses 40 69.
52. A.I. Gohari, M.Y. Mustafa, A.A. Megahed and E. Mansour (1998) Phys. Chem. Glasses 39 56.
53. D. Emin and T. Holstein (1969) Ann. Phys. (NY) 53 439.